

# Adaptive real-time femtosecond pulse shaping

D. Meshulach, D. Yelin, and Y. Silberberg

*Department of Physics of Complex Systems, The Weizmann Institute of Science, Rehovot 76100, Israel*

Received September 16, 1997

Experimental results of a practical self-learning pulse-shaping system are presented. Real-time adaptive pulse shaping of uncharacterized pulses is achieved. A cross-correlation feedback measurement of the output pulses is used by a simulated-annealing algorithm to modify the pulses iteratively toward target shapes. This scheme can readily be used for coherent control of quantum dynamics. © 1998 Optical Society of America [S0740-3224(98)01305-8]

OCIS codes: 320.0320, 320.5540, 010.1080.

## 1. INTRODUCTION

Shaping of ultrashort optical pulses into desired waveforms has been a subject of extensive work in recent years. The most successful techniques for ultrashort pulse shaping involve Fourier synthesis, where the optical field is modified by filtering of its spatially dispersed frequency components.<sup>1</sup> These techniques now allow for shaping of sub-20-fs pulses,<sup>2,3</sup> and dynamic computer-controlled pulse shaping was achieved by liquid-crystal modulators and acousto-optic modulators.<sup>4,5</sup> In all these pulse-shaping demonstrations the spectral filter was calculated according to a fully characterized input pulse, to match a desired, well-defined output pulse. However, in some situations the optical field to be used for an experiment is difficult or even impossible to be determined before hand, and consequently, the corresponding spectral filter cannot be calculated. In other situations the performance of these pulse shapers is limited by the need to constantly update the spectral filter in order to account for variations of the laser source. These limitations can be overcome by use of an adaptive approach.<sup>6-10</sup>

The ability to shape ultrashort pulses into arbitrary waveforms has inspired the research on manipulation and control of quantum-mechanical phenomena. Much theoretical work has been directed toward the design of waveforms that can drive reactions into thermally inaccessible final states.<sup>11</sup> The design of such waveforms requires complete knowledge of the Hamiltonian of the quantum system, which is generally unknown exactly even for simple systems having two or three atoms. Consequently, the filters needed to generate the desired field for specific tasks cannot be directly computed. In such situations a self-learning process can be used to adaptively tailor pulses to optimize quantum processes.

It is the purpose of this work to demonstrate experimentally, for the first time to our knowledge, a femtosecond pulse-shaping system in which a self-learning process is used to drive it to produce desired pulse shapes. In our previous work<sup>10</sup> we have shown that adaptive techniques can be used successfully to compress femtosecond pulses, by tailoring of the spectral phase of the incoming pulses, to cancel any spectral-phase distortions. In this work we generalize the technique of adaptive pulse compression to

adaptive pulse shaping, to generate almost arbitrary waveforms. While here we use a predefined pulse shape as our target, in principle a measurement of a physical process induced by the shaped pulses, such as second-harmonic generation as in Ref. 10, or fluorescence, can be used as a feedback signal to drive the system to perform a specific task.

## 2. THEORY

Adaptive ultrashort pulse compression and shaping involve the use of a dynamic pulse shaper and a feedback measurement. In general, a computer is used to optimize a cost function that indicates the adequacy of the output pulses to perform a desired task. In our adaptive pulse-shaping scheme the input pulses, which need not be characterized, are modified iteratively to match desired pulse shapes by minimization of a cost function that indicates the deviation of the output pulses from the desired shapes. As in our previous work on adaptive compression,<sup>10</sup> we used a programmable pulse shaper that allows for independent control of the individual spectral components of the incoming pulses, to realize almost arbitrary waveforms. A cross-correlation measurement of the output pulses was used as a feedback to evaluate a cost function that was minimized by a simulated-annealing optimization procedure.<sup>9</sup> In this work we characterized the output pulses by an intensity cross-correlation measurement, and therefore this scheme was insensitive to the phase structure of the output field.

### A. Optimization of the Phase Filter

We used a simulated-annealing algorithm similar to that described in our previous work,<sup>9,10</sup> to optimize the pixelized spectral phase mask of our femtosecond pulse shaper (see Section 3). The optimization procedure, illustrated in Fig. 1, begins by setting the predetermined number of iterations  $N$ , and by assigning a zero phase delay to an initial trial phase vector  $\Phi$ . In each iteration a random phase change vector  $\delta\Phi$  is generated according to

$$\delta\Phi = \alpha \left( 1 - \frac{i}{N} \right) \mathbf{r}, \quad (2.1)$$

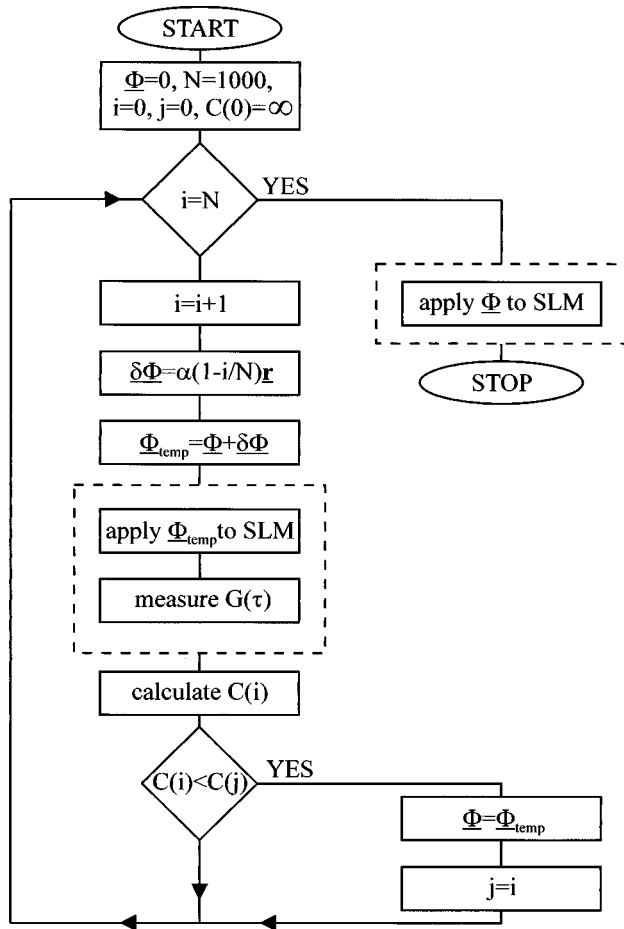


Fig. 1. Optimization procedure for adaptive pulse shaping. The dashed boxes describe operations that are performed by the experimental optical setup. In each iteration a random phase change vector is generated and added to the current phase vector to form a trial phase filter, which is applied to the SLM. The output shaped pulse is measured, a cost is calculated, and the change is accepted if the cost is smaller than that of the last accepted change, and rejected otherwise.

where  $i$  is the iteration number,  $\mathbf{r}$  is a random variable vector, whose elements are uniformly distributed between  $-\pi/2$  and  $\pi/2$ , and  $\alpha$  is an adjustable constant parameter. Both  $N$  and  $\alpha$  are set to improve the rate of convergence. The random phase change vector  $\delta\Phi$  is added to the current phase vector  $\Phi$ , to form a trial phase solution vector  $\Phi_{\text{temp}}$ , and this phase vector is applied to the programmable pulse shaper, to generate the shaped output pulses. The intensity cross-correlation signal of the output shaped pulse  $G^{(i)}(\tau)$  is then measured:

$$G^{(i)}(\tau) = \int I_{\text{out}}^{(i)}(t) I_{\text{ref}}(t + \tau) dt, \quad (2.2)$$

where  $I_{\text{out}}^{(i)}(t)$  and  $I_{\text{ref}}(t)$  are the intensities of the output pulse and a short reference pulse obtained directly from the laser, respectively. Next, the cost  $C^{(i)}$  is calculated, as described in the following subsection. The new phase change is always accepted if the new cost is smaller than that of the last accepted phase change, and rejected otherwise.

## B. Cost Functions

The simulated-annealing algorithm, used for the optimization of the phase filter, requires the use of a cost function, which provides a measure of the deviation of the shaped pulses from the target shapes. In defining the cost function, considerations such as the target-shape symmetry, limitations imposed by the experimental setup, and convergence rate of the optimization procedure should be taken into account. For this work we investigated the use of three cost functions. First, we calculate the intensity cross correlation between the desired output pulse and a short reference pulse, to form the target shape  $G_{\text{tar}}(\tau)$ . A straightforward definition for the cost function is

$$C^{(i)} = \int |G^{(i)}(\tau) - G_{\text{tar}}(\tau)| d\tau. \quad (2.3)$$

The minimization of this cost function requires that the shaped pulse matches the target shape. However, Eq. (2.3) does not allow for any temporal shifts between the shaped pulse and the target shape, which are of no importance in most experimental situations. This constraint reduces the solution space and hence the rate of convergence. Furthermore, mechanical instabilities such as synchronization jitter of the cross-correlation measurement may significantly alter the cost and prevent the process from converging. A time-invariant cost function can be defined as follows:

$$C^{(i)} = \min_{|\delta\tau| < T} \int |G^{(i)}(\tau + \delta\tau) - G_{\text{tar}}(\tau)| d\tau, \quad (2.4)$$

where  $\delta\tau$  is a time shift, and  $T$  is a small time window. The cost function, given by Eq. (2.4), overcomes the time-invariance problem, but introduces additional complexity to the optimization algorithm, and may increase the overall time needed for the optimization process.

We have also used an alternative definition for a time-invariant cost function:

$$C^{(i)} = \int ||\mathcal{F}^{(i)}(\omega) - \mathcal{F}_{\text{tar}}(\omega)|| d\omega, \quad (2.5)$$

where  $\mathcal{F}^{(i)}(\omega)$  and  $\mathcal{F}_{\text{tar}}(\omega)$  are the Fourier transforms of  $G^{(i)}(\tau)$  and  $G_{\text{tar}}(\tau)$ , respectively. The time-invariant property simply follows from the fact that the power spectrum of a signal is identical to the power spectrum of its time-shifted replica. However, since both  $G_{\text{tar}}(\tau)$  and  $G_{\text{tar}}(-\tau)$  have the same power spectrum, the algorithm might converge to a time-reversed version of the target shape, as we have observed in some experiments. The cost function given by Eq. (2.5) is suited for symmetrical target shapes.

## 3. EXPERIMENTAL RESULTS

The layout of our experimental setup for adaptive pulse shaping is shown in Fig. 2. The setup is composed of a programmable pulse shaper, a cross-correlation measurement arrangement, a digital oscilloscope, and a computer used for calculating and updating the spectral filter. The femtosecond pulse source for the experiment was a mode-locked Ti:sapphire laser, which produced 27-fs FWHM

Fourier-limited  $\text{sech}^2$  intensity pulses, centered at 800 nm. The programmable  $4-f$  pulse shaper<sup>1</sup> was composed of a pair of diffraction gratings with 1200 lines/mm and a pair of achromat lenses with a 100-mm focal length. A programmable one-dimensional liquid-crystal spatial light modulator (SLM) array (SLM-256, Cambridge Research & Instrumentation, Inc.) was placed at the Fourier plane of the shaper and was used as an updatable filter for spectral manipulation of the incoming pulses. This SLM allows for independent control of the phase and the amplitude for each of its 128 pixels,<sup>12</sup> although in this work it was used as a phase-only filter.<sup>13</sup> The width of each pixel was  $97 \mu\text{m}$ , the interpixel gap was  $3 \mu\text{m}$ , and the spot size at the Fourier plane was  $\sim 80 \mu\text{m}$ . A real-time background-free intensity cross-correlation measurement was performed to characterize the output pulses. We achieved this by focusing the output pulses and the short reference pulse, obtained directly from the laser, using a lens with 50-mm focal length, onto a 100- $\mu\text{m}$ -thick frequency-doubling  $\beta$  barium borate crystal. The second-harmonic signal was detected by a photomultiplier, sampled by a digital oscilloscope, and displayed in real-time. A computer served for reading this signal, for evaluating the cost function, for optimizing the spectral filter, and for updating the SLM. To demonstrate the potential of adaptive shaping, we numerically generated a variety of desired pulse shapes, and the intensity distribution of each of them was numerically cross correlated with a 27-fs  $\text{sech}^2$  intensity pulse, to form target shapes. We then closed the feedback loop, and monitored, during each run, the evolution of the cost function as the process progressed.

The experimentally obtained cross-correlation measurements of the shaped output pulses and the target shapes for three different cases are shown in Fig. 3. The target shapes (dashed), correspond to (a) a sequence of

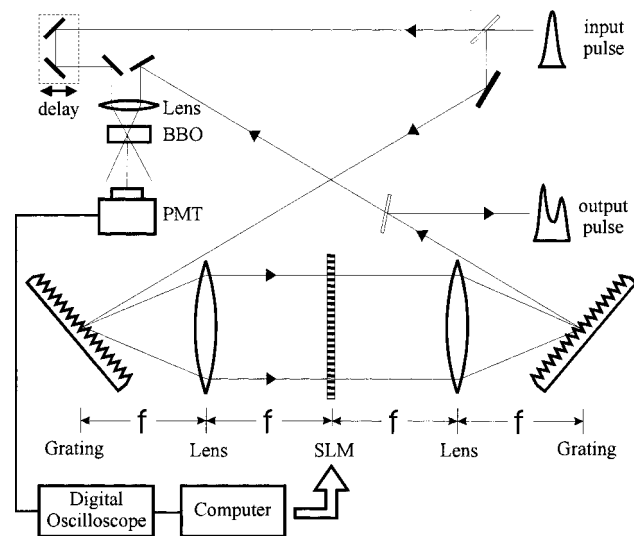


Fig. 2. Experimental setup for adaptive pulse shaping. The setup consists of a  $4-f$  pulse shaper, a programmable liquid-crystal SLM, a background-free intensity cross-correlation arrangement, a digital oscilloscope, and a computer. The computer was used for acquiring the cross-correlation measurement, for calculating the cost function, and for updating the spectral filter of the SLM accordingly.

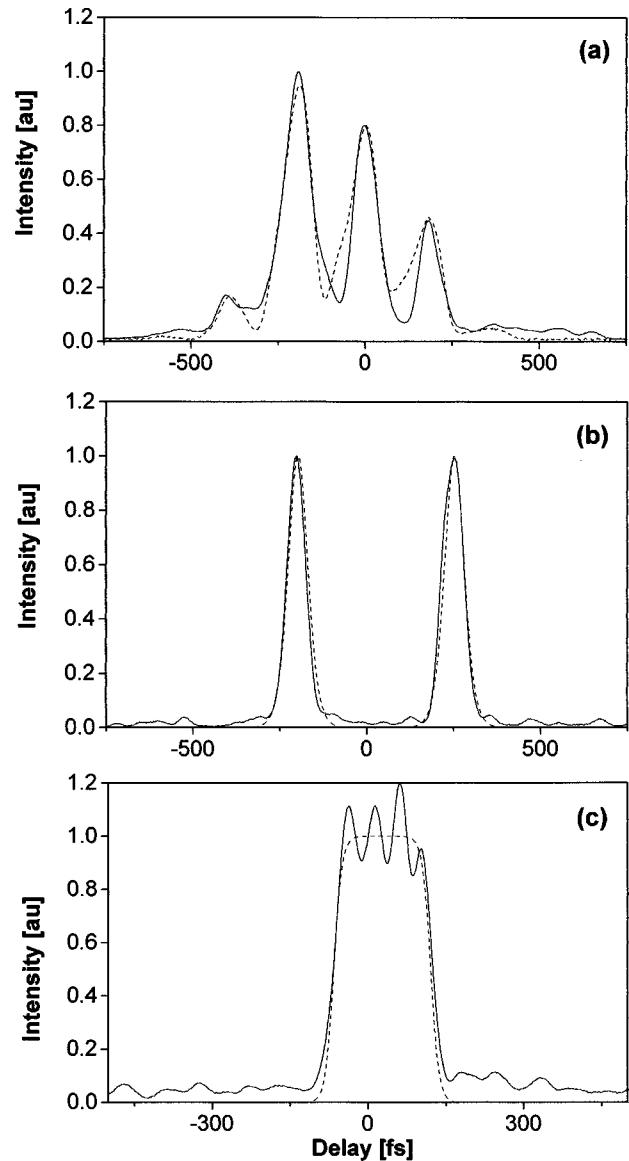


Fig. 3. Experimental cross-correlation signals of the shaped pulses (solid) and the target signals (dashed): (a) A sequence of few nonidentical features. (b) A pulse doublet, each pulse of 54-fs-long duration, separated by 450 fs. (c) A square pulse of 190-fs-long duration. The results were obtained by a simulated-annealing algorithm after 1000 iterations.

few nonidentical features, (b) a pulse doublet, each pulse of 54-fs-long duration, separated by 450 fs, and (c) a square pulse of 190-fs-long duration. The corresponding shaped output pulses, shown in Figs. 3(a)–3(c) (solid), were obtained by use of the simulated-annealing algorithm with 1000 iterations, and the cost was calculated according to Eq. (2.5) for case (a) and according to Eq. (2.4) for cases (b) and (c). As can be verified by comparing the shaped pulses with the target shapes, the location of the features of the output pulses, their duration, and their heights well match those of the target shapes. However, in case (c) the top of the shaped pulse is not flat. This result is mainly attributed to fundamental limitations of phase-only filtering, since it is well known, in general, that phase-only filtering can be used only to approximate desired pulses. Indeed, our experimental results

agree with the results of square pulse shaping obtained by phase-only filtering reported in Ref. 13. In order to analyze the performance of our adaptive pulse-shaping scheme, as well as to provide an insight to the adaptive shaping process, we performed simulations of the adaptive process and calculated the shaping of pulses into the same target shapes used in the experiment. Figure 4 presents the target shapes (dashed) and the corresponding calculated shaped output pulses (solid). These results were obtained by use of the simulated-annealing algorithm with 1000 iterations. Finally, as a typical example, we present in Fig. 5 the convergence process as reflected through the decrease of the cost function for the shaping procedure toward the shape shown in Fig. 3(a). Interestingly, this type of convergence was typical for all runs, and it was also observed in the numerical simulations.

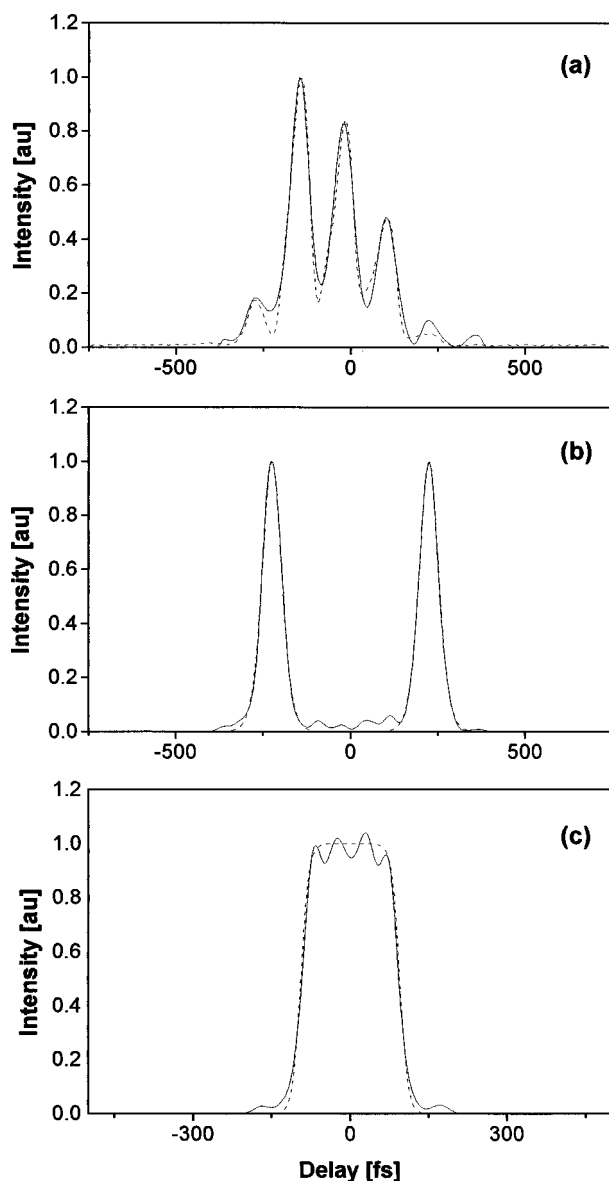


Fig. 4. Calculated cross-correlation signals of the shaped pulses (solid) and the target signals (dashed), corresponding to the experimental results shown in Figs. 3(a)–3(c).

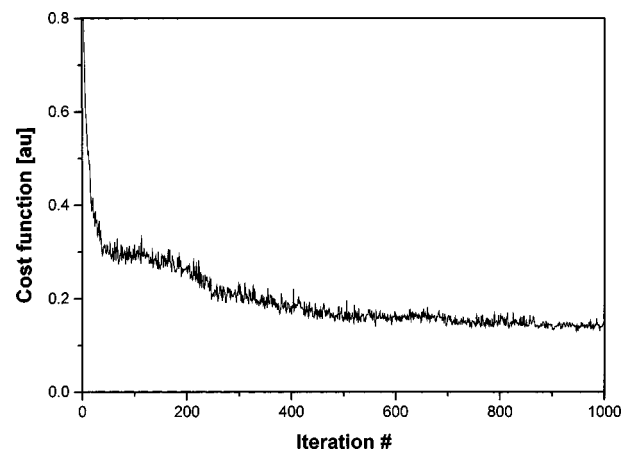


Fig. 5. Convergence of the cost function for the case of adaptive shaping, where the final shaped pulse is shown in Fig. 3(a).

Although the cross correlation of the shaped pulses well approximates the target shapes, the results should be carefully interpreted. In this work the pulses were adaptively shaped to approximate the intensity cross correlation between a desired pulse and a short reference pulse. Consequently, the shaped pulses were characterized by their intensity distribution, and not by their complex field. However, this is not a fundamental limitation of the adaptive pulse-shaping approach. Essentially, any real-time technique for full characterization of the shaped pulses, such as real-time frequency-resolved optical gating<sup>14</sup> or real-time temporal analysis by dispersing a pair of light  $e$  fields<sup>15</sup> can be used to calculate a cost function to approximate any complex target field distribution, rather than an intensity distribution. Such complete control of temporal amplitude and phase requires both amplitude and phase modulation of the spectral components, which doubles the degrees of freedom for optimization.

Adaptive pulse shaping by this SLM is subject to a number of limitations, as we have already discussed in our adaptive compression demonstration.<sup>10</sup> Since spectral filtering is accomplished by control over 128 discrete pixels of the SLM, continuous filters cannot be realized, and strong spectral phase variations cannot be applied. Furthermore, owing to the pixilation, some modulation of the spectrum was observed. As a result, low-intensity pulses separated by  $\sim 3$  ps from the shaped pulse were measured. Although these pulses were small, they could interfere with the pulse when its features overlap with them. Consequently, pulse shaping by our SLM in this configuration was limited to generate shaped pulses within an  $\sim 3$ -ps temporal window. An important issue regarding any practical implementation of the adaptive scheme is the overall time needed for the process. In this work the bottleneck of the process was the updating time of the SLM, which was  $\sim 500$  ms, limited by the electronics driver of the SLM, so that the time needed for a single iteration was  $\sim 1$  s. In this work, 1000 iterations were performed at each run, setting the overall time needed for the shaping process to  $\sim 15$  min. The update time can be significantly reduced with higher update rates and faster SLM's.

#### 4. CONCLUSIONS

In summary, we have shown first experimental results of adaptive femtosecond pulse shaping. A practical self-learning scheme was used for shaping of uncharacterized pulses into desired waveforms. We expect that this technique, with appropriate feedback signals, will play an important role in the field of coherent control of quantum dynamics, by use of the experimental setup as an analog computer to exactly solve Schrödinger's equation in real time.

#### REFERENCES

1. A. M. Weiner and J. P. Heritage, *Rev. Phys. Appl.* **22**, 1619 (1987).
2. D. H. Reitze, A. M. Weiner, and D. E. Leaird, *Appl. Phys. Lett.* **61**, 1260 (1992).
3. A. Efimov, C. Schaffer, and D. H. Reitze, *J. Opt. Soc. Am. B* **12**, 1968 (1995).
4. A. M. Weiner, D. E. Leaird, J. S. Patel, and J. R. Wullert, *Opt. Lett.* **15**, 326 (1990).
5. C. W. Hillegas, J. X. Tull, D. Goswami, D. Strickland, and W. S. Warren, *Opt. Lett.* **19**, 737 (1994).
6. R. S. Judson and H. Rabitz, *Phys. Rev. Lett.* **68**, 1500 (1992).
7. W. S. Warren, H. Rabitz, and M. Dahleh, *Science* **259**, 1581 (1993).
8. A. M. Weiner, *Prog. Quantum. Electron.* **19**, 161 (1995).
9. D. Meshulach, D. Yelin, and Y. Silberberg, *Opt. Commun.* **138**, 345 (1997).
10. D. Meshulach, D. Yelin, and Y. Silberberg, "Adaptive compression of femtosecond pulses," presented at Ultrafast Optics 1997 Meeting of the Optical Society of America, Monterey, Calif., session WPD-1, August 4-7, 1997; D. Yelin, D. Meshulach, and Y. Silberberg, *Opt. Lett.* **22**, 1793 (1997).
11. S. Shi and H. Rabitz, *J. Chem. Phys.* **92**, 364 (1990).
12. M. M. Wefers and K. A. Nelson, *Opt. Lett.* **20**, 1047 (1995).
13. A. M. Weiner, S. Oudin, D. E. Leaird, and D. H. Reitze, *J. Opt. Soc. Am. A* **10**, 1112 (1993).
14. D. Kane, "Real-time inversion of frequency-resolved optical gating (FROG) spectrograms: A femtosecond oscilloscope," presented at Ultrafast Optics 1997 Meeting of the Optical Society of America, Monterey, Calif., session MA-3, August 4-7, 1997.
15. D. N. Fittinghoff, J. L. Bowie, N. Sweetser, R. T. Jennings, M. A. Krumbügel, K. W. DeLong, R. Trebino, and I. A. Walsmley, *Opt. Lett.* **21**, 884 (1996).